Available online at www.sciencedirect.com

SCIENCE DIRECT®

International Journal of Mass Spectrometry 233 (2004) 385–394

International Journal of Mass Spectrometry

www.elsevier.com/locate/ijms

Parity violating effects in the molecular anion $CBrClF^-$

Jürgen Stohner*

Zürich University for Applied Sciences ZHW, Institute of Chemistry and Biotechnology ICB, P.O. Box 805,
Technikumstrasse 9 CH-8401 Winterthur, Switzerland

Received 14 January 2004; accepted 15 January 2004

This paper is dedicated to Tilmann Märk on the occasion of his 60th birthday.

Abstract

We examine the influence of molecular parity violation on relative vibrational frequency shifts in the carbanion $CBrClF^-$. The parity violating potential has been calculated following the method of Berger and Quack [J. Chem. Phys. 112 (2000) 3148] using a multi-configurational linear response approach. The vibrational frequency shifts have been determined in the separable harmonic (SHAA) and anharmonic (SAAA) adiabatic approximation. We find that $CBrClF^-$ shows larger (in absolute magnitude) relative frequency shifts compared to the neutral CHBrClF. The relative frequency shifts depend strongly on the vibrational wavefunction used to determine the expectation value of the parity violating potential. We determined also the energetic stability of $CBrClF^-$ with respect to electron detachment, Br^- and Cl^- abstraction and protonation to form CHBrClF.

Keywords: $CBrClF^-$; CHBrClF; Frequency shifts; Parity violation; Molecular ions

1. Introduction

Singly charged atomic and molecular ions play an important role in many areas of science and technology, ranging from interstellar chemistry, ion kinetics on surfaces, organic chemistry, radiocarbon dating methods to the investigation of enzymatic activities [1–10] (and references therein), to mention just a few. Gaseous ions are also very well suited for high precision frequency measurements due to the possibility to confine them stationary in ion traps under almost single particle conditions [11]. Optical frequency standards that are based on narrow absorption bands in laser-cooled and trapped single ions are stable and competitive to other optical high frequency standards through their reduced line broadening [12]. This is important for atomic clocks, for example, which are based on observing spectroscopic transitions in gases [13,14], where the achievable resolution is limited through line broadening mechanisms.

The violation of mirror image symmetry (left–right asymmetry or parity violation in quantum mechanical language) in nuclear physics is well established since about 1957 [15,16]. For instance, the weak interaction is responsible for β-decay which changes the charge of the nucleus and simultaneously emits an electron or a positron. Fermi described this β-decay phenomenologically by introducing a charged current [17]. Zel'dovich discussed neutral weak currents and their influence on electron–nucleon interactions in atoms [18]. Glashow, Weinberg, and Salam (GWS) unified the weak and the electromagnetic interactions, known as the electroweak part of the Standard Model, by introducing two charged (W^+, W^-), and one neutral Z^0 heavy boson which mediate the weak interactions. Z^0 is responsible for the neutral weak current interaction. Re-normalizability of GWS was conjectured and later proven by t'Hooft and Veltman in 1971. The first precision measurements on parity violation in atoms as caused by the neutral weak current followed the theoretical investigations of the Bouchiats (for a review, see [19]).

Parity violation in atoms is a very small effect which requires ultrahigh precision measurements, however, it is scaling approximately with Z^3, where Z is the nuclear charge. Z-enhanced parity violating transitions have been observed in a number of atoms (see [20]). Trapped atomic ions have

---

* Present address: Academic Visitor to ETH Zürich (Hönggerberg) Physical Chemistry, HCI E227, Wolfgang-Pauli-Str. 10, CH-8093 Zurich, Switzerland. Tel.: +41-1-632-6012; fax: +41-1-632-1021.

E-mail addresses: just@ir.phys.chem.ethz.ch, sth@zhwin.ch (J. Stohner).

1387-3806/$ – see front matter © 2004 Elsevier B.V. All rights reserved.
doi:10.1016/j.ijms.2004.01.015

been used to investigate electromagnetic and weak interactions [21,22]. Soon after the discovery of parity violation in nuclear physics, it was realized that interesting consequences arise in molecular physics. Parity violation induces a very small energy difference between the left- and right-handed molecule of a chiral compound (enantiomers) [23–25] with possible consequences for the homochirality in nature (for extensive reviews, see also [26,27] and references therein). The latter connection is still subject to discussion and we refer to recent reviews on that matter [26,28,29].

Molecular parity violation has still not been observed experimentally, although proposals for spectroscopic experiments do exist for a while ([27,30,31]). One might distinguish three types of experimental approaches to molecular parity violation. In a spectroscopic experiment carried out on enantiomerically pure substances one would try to measure frequency splittings between left- and right-handed molecules in a direct spectroscopic (time-independent) manner. This requires a precise knowledge of the molecular spectroscopic Hamiltonian which includes all relevant terms and a careful analysis of potentially observed line shifts. This approach has been chosen exclusively in the past (see Table 1). The interpretation, however, is very difficult and subject to misinterpretations due to systematic or statistical flaws inherent in the experimental setup or in the theory adopted to verify potentially observed frequency shifts caused by parity violation. None of those time-independent experiments focusing on the direct observation of line shifts succeeded so far [25,32–36]. When parity violation dominates over tunneling (high barrier limit), a different strategy described in [27,30] would use a time-dependent more direct approach and study the time resolved transformation of an initial state with well defined parity to a state of opposite parity in a pump-probe arrangement [27,30]. This would allow one to determine the parity violating energy difference $\Delta_{\mathrm{pv}}E$ between enantiomers, which is proportional to the heat of stereomutation $\Delta_{\mathrm{pv}}H_0^{\circ}$.

Yet another approach suggests to measure parity mixing by quantum beats of optical rotation [37,38] in the intermediate regime where tunneling and parity violation compete and thus is limited to fairly special intermediate cases. Those time-dependent experiments are, however, extremely difficult and although suggested quite some time ago, they have not yet been realized. The interpretation of time-dependent signals is believed to be straightforward whereas the interpretation of the results from line shift measurements is more involved. A third type of experiment focuses on the observation of macroscopic quantities like differences in specific heat capacities, thermodynamic quantities related to phase transitions, and alike. This type of experiment is without doubt the most difficult to interpret and to unequivocally rule out any other effect that might indicate parity violation (see also the discussion in [26]).

Since the discovery in Martin Quack's group that parity violating energy differences are much larger than previously anticipated based on early ab initio calculations [39–41] by using more adequate ab initio methods [42–45], an increased interest in this fundamental topic emerged and triggered an improvement of computational methods. Quantum chemical methods currently available are Hartree–Fock [39,40], configuration interaction (singles) [42–44], random-phase approximation (RPA) [46] (not multi-configurational), multi-configurational linear response (complete-active space self-consistent field (CASSCF), RPA CISDTQ, etc.) [45], relativistic Dirac–Hartree–Fock (DHF) [47], and density functional theory (DFT) [48]. Additionally, all required equations have been derived which would be needed to investigate parity violating interactions in atoms and molecules within the coupled cluster of singles and doubles linear response approach [49], however, no numerical results have so far been published nor has the question of parity violation specifically been addressed therein. The basic general theory has been reviewed in [43] and a recent extensive review of the theory as well as numerical results on the determination of molecular parity violation energies is provided in [50]. Strategies on how to compute molecular observables influenced by parity violation like rotational [51,52] and vibrational frequency shifts [51–57], equilibrium constants and thermodynamic quantities [58], as well as NMR chemical shifts [59–62] have been described. Reliable calculations are needed to search for molecular systems that are promising candidates for an experimental investigation of molecular parity violation.

Here, a new aspect concerns the use of molecular (trapped) ions [25] for a possible experimental investigation. Because of parity mixing by electric fields of the traps this might, however, add further complications (see [26]) to already proposed (but difficult to realize) experimental

Table 1
Experimental attempts to measure parity violating effects in molecules with the aid of time-independent molecular spectroscopy

Molecule	Limit, technique	Year [reference]
CHBrClF	$\Delta\tilde{\nu} \approx 10^{-3}\,\mathrm{cm}^{-1}$, vibrational spectroscopy	1976 [32]
$C_{10}H_{16}O$, camphor	$\Delta\tilde{\nu} \approx 10^{-5}\,\mathrm{cm}^{-1}$, (ro)vibrational spectroscopy (saturation, dip)	1977 [110]
CHBrClF	$\Delta\tilde{\nu} \approx 4 \times 10^{-4}\,\mathrm{cm}^{-1}$, rotational spectroscopy, jet expansion	1997 [33]
C_2H_3FO, C_2HD_2FO, fluorooxirane	$\Delta\tilde{\nu} \approx 1.6 \times 10^{-3}\,\mathrm{cm}^{-1}$, rotational spectroscopy, cell (300 K)	1997 [111]
CHBrClF	$\Delta\tilde{\nu} \approx 2.5 \times 10^{-10}\,\mathrm{cm}^{-1}$, rotational spectroscopy, hyperfine	1999 [34], 2002 [36]

The quantity $\Delta\tilde{\nu}$ gives the achieved experimental resolution and is an upper limit for the anticipated frequency shift for CHBrClF, camphor ($C_{10}H_{16}O$), fluorooxirane (C_2H_3FO), and dideutero fluoroxirane (C_2HD_2FO) which is calculated from the corresponding relative frequency shifts $\Delta\tilde{\nu}/\nu$ (given in the references) for a frequency of $\tilde{\nu} = 1000\,\mathrm{cm}^{-1}$.

schemes which are designed to unequivocally measure, identify, and analyze molecular parity violation-induced effects [27,30,31,38], as described above. Computational investigations might therefore again be useful as a first step towards this goal. Only a small number of molecular ions have been investigated theoretically and the only quantity related to molecular parity violation which has been determined was the parity violation-induced energy difference $\Delta_{\text{pv}}E$ between enantiomers of: CHClFO^-, CHBrFO^-, CHFLi^- [63], PNH_3FBr^+ [64], $[\text{O}_8]^{2-}$, $[\text{S}_6]^{2-}$ [65], and HOClH^+ [66].

After a short introduction to molecular parity violation, we will present results on vibrational frequency shifts caused by parity violation for some selected vibrational modes of the anion CBrClF^-. The neutral isotopomers CHBrClF and CDBrClF have been investigated in detail before (see [58] for a review) and we summarize the findings briefly: We determined relative frequency shifts $\Delta_{\text{pv}}\tilde{\nu}/\tilde{\nu}$ for the nine vibrational modes of CHBrClF and CDBrClF. Various levels of approximation have been discussed: (i) In a first approximation, we treated the vibrational motion as purely harmonic (separable harmonic adiabatic approximation (SHAA)) and determined relative vibrational frequency shifts from a coordinate-dependent parity violating potential for each vibrational mode separately (that is uncoupled) [52,53]. By considering anharmonic contributions (separable anharmonic adiabatic approximation (SAAA)) to the vibrational motion we found (ii) that the relative frequency shifts may change sign as well as magnitude compared to (i) which leads to the conclusion that anharmonic contributions to the frequency shifts are very important [51,56]. Strong multi-dimensional anharmonic coupling between various vibrational modes influence the relative frequency shifts considerably as well, which has been demonstrated recently for CDBrClF with the aid of four-dimensional vibrational and parity violating potential energy hypersurfaces [67].

2. Theory

2.1. Ab initio calculations

Geometries and harmonic vibrational frequencies of (S)-CBrClF^- have been determined with second-order Moller–Plesset perturbation theory (MP2) and DFT employing various basis sets [68]. DFT calculations have been performed with the hybrid functional B3LYP. The structures have been fully optimized and the stationary points are classified as minimum structures with all vibrational frequencies real. Where appropriate, unrestricted wavefunctions have been used in the DFT and MP2 calculations; in the latter case, energies have then been obtained after spin projection. We used Gaussian 98 for the ab initio exploration of the parity conserving potential energy surface [69]. Upon diagonalizing the mass weighted Cartesian force constant matrix, we obtain dimensionless reduced normal coordinates q_i for each vibrational mode i [51,52,67]. A numerical value of q_i different from zero is connected with a displacement from the equilibrium position ($q_i = 0$) and therefore defines a new Cartesian geometry. At each geometry obtained by varying q_i, we calculate the pure vibrational parity conserving potential as well as the parity violating potential. The latter has been calculated with a local version including parity violation [45] of the DALTON package [70]. The parity violating potential is fitted to a polynomial expansion whereas the vibrational potential is spline interpolated upon solving the Schrödinger equation on a grid [71–75]. From the eigenvalues and vibrational wavefunctions, we determine relative frequency shifts as outlined below.

2.2. Electroweak molecular parity violation

The parity violating Hamiltonian for stable atomic and molecular systems have been derived within the Standard Model of electroweak interaction [19,40,43,76] (and references therein) based on the neutral current for the electron–nucleus potential, which is estimated to be much larger than the electron–electron potential [76]. The parity violating weak interaction is a contact-like interaction locally confined to the position of the nucleus at chemically relevant energies.

In a non-relativistic approximation, three contributions for each electron i have been considered relevant in order to compute the parity violating interaction $H_{\text{pv}}^{\text{eN}}$, namely [43,59–61]:

$$H_{\text{pv}}^{\text{eN}} = \frac{G_F}{2\sqrt{2}m_e c}(H_{\text{pv}}^{(1)} + H_{\text{pv}}^{(2)} + H_{\text{pv}}^{(3)}) \quad (1)$$

where m_e is electron mass; c is speed of light; $G_F \approx 1.43586\times10^{-62}\,\text{J m}^3$ is Fermi weak coupling constant which is derived from the muon lifetime τ_μ [77,78]. The individual terms are as follows:

$$H_{\text{pv}}^{(1)} = Q_a\vec{s}\cdot[\vec{p}, \delta(\vec{r}-\vec{r}(a))]_+ \quad (2)$$

$$H_{\text{pv}}^{(2)} = -4\lambda_a(1-4\sin^2(\theta_W))(\vec{s}\cdot[\vec{p}, \delta(\vec{r}-\vec{r}(a))]_+)(\vec{s}\cdot\vec{I}(a)) \quad (3)$$

$$H_{\text{pv}}^{(3)} = e\vec{s}\cdot(\vec{B}_0\times(\vec{r}(a)-\vec{r}_{(\text{G.O.})})) \cdot\{Q_a - 4\lambda_a(1-4\sin^2(\theta_W))\vec{s}\cdot\vec{I}(a)\} \quad (4)$$

where $\vec{s}$ is electron spin, $\vec{p}$ is the electron linear momentum, e is the elementary charge, $\delta(\vec{r}-\vec{r}(a))$ is 3-dimensional Dirac delta distribution confining the interaction locally to the (point) nuclear position, $\vec{r}(a)$ is the position vector of the nucleus $\vec{r}_{(\text{G.O.})}$ is the position vector of the gauge origin, and $[\ldots]_+$ denotes anti-commutator. The weak charge is (e.g., upon neglecting radiative corrections) approximately given by

$$Q_a \approx (1-4\sin^2(\theta_W))Z_a - N_a \quad (5)$$

where N_a is the neutron number of nucleus a; Z_a is the nuclear charge, and θ_W the Weinberg angle with $\sin^2(\theta_W) \approx 0.2319$ [78], and λ_a is a nuclear parameter close to 1 [50,59]. $H_{\rm pv}^{(2)}$ and $H_{\rm pv}^{(3)}$ depend on nuclear spin $\vec{I}(a)$. $H_{\rm pv}^{(3)}$ has to be included if an external static magnetic flux density $\vec{B}_0$ is present. In atomic physics, however, nuclear spin-dependence is considered small and therefore usually neglected which then leads to $H_{\rm pv}^{\rm eN} \approx G_F/(2\sqrt{2}m_{\rm e}c)H_{\rm pv}^{(1)}$.

Nuclear spin-dependent effects have so far also been neglected in molecular parity violation except in cases where one is specifically interested in observables that depend on nuclear spin, as for example the NMR chemical shift [59–62]. The nuclear spin-dependent terms in $H_{\rm pv}^{(2)}$ and $H_{\rm pv}^{(3)}$ are weighted by a factor $(1 - 4\sin^2(\theta_W)) \approx 0.07$ which is rather small. Thus, we might neglect in a first approximation the nuclear spin-dependent terms in the molecular parity violating Hamiltonian which itself is obtained from the atomic Hamiltonisan by a simple sum over all nuclei and electrons i (see [40,43,45,59–61,65] and references therein) resulting in

$$H_{\rm pv} \approx \frac{G_F}{2\sqrt{2}mc}\sum_a Q_a \sum_i [[\vec{p}(i)\cdot\vec{s}(i), \delta(\vec{r}(i)-\vec{r}(a))]_+ + e\vec{s}(i)\cdot(\vec{B}_0 \times (\vec{r}(a)-\vec{r}_{(\rm G.O.)}))] \tag{6}$$

The first term in Eq. (6) has been used in the non-relativistic (or rather semi-relativistic) limit to calculate parity violation in molecules in absence of an external magnetic field [39,40,43,45,65,79]. In the presence of uniform external magnetic fields, the second term in Eq. (6) depending on the magnetic flux density $\vec{B}_0$ would have to be included. However, in the current investigation we neglect the $\vec{B}_0$-dependent term.

In a recent investigation on gas-phase NMR [61], it has been shown that the parity violation-induced chemical shielding and a corresponding frequency shift between enantiomers of H_2O_2, is on the order of about 10 μHz (for a flux density of $B_0 \approx 11$ T, which is certainly larger than those employed in magnetic traps). This value is much smaller than the parity violation-induced energy difference ($\Delta_{\rm pv}E/h$) of about 5 mHz and still smaller than the anticipated parity violation-induced vibrational frequency shift. From the series H_2O_2, H_2S_2 and H_2Se_2 is has been concluded that nuclear spin-dependent contributions to parity violation depend less strongly on the nuclear charge Z^n with $n = 2, 3$, whereas the parity violating effect resulting from the first part of Eq. (6) has $n = 5\pm1$ [61,80,81]. The larger Z, the smaller is the contribution of the nuclear spin-dependent term compared to the nuclear spin-independent term. For our purpose (with bromine as heavy nucleus which contributes most to parity violation), it seems therefore justified to neglect the nuclear spin-dependent term. This, however, needs a more detailed investigation in the future.

2.3. Molecular spectropscopic Hamiltonian

A general procedure to determine the effect of molecular parity violation on spectroscopic observables like line positions has been described in detail [67] and we summarize here only briefly. The molecular Hamiltonian $\hat{H}_{\rm mol}$ is split into a parity conserving or parity even part, $\hat{H}_0$ (usually the Born Oppen-heimer approximation to the vibrational–rotational motion in the ground electronic state) and the parity violating or parity odd part, $\hat{H}_{\rm pv}$:

$$\hat{H}_{\rm mol} = \hat{H}_0 + \hat{H}_{\rm pv} = \hat{T}_0(\vec{q}) + \hat{V}_0(\vec{q}) + \hat{V}_{\rm pv}(\vec{q}) \tag{7}$$

with the kinetic and potential energies $\hat{T}$ and $\hat{V}$, respectively. In a first step one solves the pure (ro)vibrational problem

$$(\hat{T}_0 + \hat{V}_0)|\,v\rangle = E_v^{(0)}|\,v\rangle \tag{8}$$

where $E_v^{(0)}$ denotes the vth eigenvalue and $|\,v\rangle$ is the corresponding eigenfunction of the parity conserving Hamiltonian; $\vec{q}$ is a shorthand notation for the collection of the $3N - 6 = 6$ (N is the number of atoms) vibrational reduced normal coordinates q_1–q_6; v in Eq. (9) counts the eigenfunctions and eigenenergies. Since the parity violating potential $V_{\rm pv}$ is very small, one can make use of low order perturbation theory. An estimate of the anharmonic eigenenergy of the vibrational molecular Hamiltonian including the parity violating potential energy, E_v, is thus obtained from the zeroth order energy $E_v^{(0)}$ (without $V_{\rm pv}$ $(\vec{q})$ present) by

$$E_v \approx E_v^{(0)} + E_v^{(1)} \approx E_v^{(0)} + \langle v|\,V_{\rm pv}(\vec{q})\,|v\rangle \tag{9}$$

and $E_v^{(1)}$ is the first-order perturbation correction to the eigenenergy of the zeroth order Hamiltonian $\hat{H}_0$ without parity violation present; this correction corresponds to the expectation value of the parity violating potential.

Different levels of approximations can be applied to the kinetic energy operator $\hat{T}$ or the potential energy $\hat{V}$ of the Schrödinger equation. We consider vibration and rotation decoupled and investigate here only the vibrational problem. In the SHAA, the relative frequency shift $\Delta_{\rm pv}\tilde{\omega}_i/\tilde{\omega}_i$ is related to the parity violation potential parameter $\tilde{p}_2$ that depends quadratically on the reduced normal coordinate as

$$\frac{\Delta_{\rm pv}\tilde{\omega}_i}{\tilde{\omega}_i} \approx \frac{2\tilde{p}_2}{\tilde{\omega}_i} \tag{10}$$

Relative frequency shifts in the SAAA for corresponding lines of the R and S enantiomers in mode j are given by [51,52,58,67].

$$\frac{\Delta_{\rm pv}\tilde{\nu}_j^{\rm ul}}{\tilde{\nu}_j^{\rm ul}} \approx \frac{2\left(\left\langle v_j^{\rm u}|\,V_{\rm pv}/hc\,|v_j^{\rm u}\right\rangle - \left\langle v_j^{\rm l}|V_{\rm pv}/hc|v_j^{\rm l}\right\rangle\right)}{(E_{{\rm u},j}^0 - E_{{\rm l},j}^0)/(hc)} \tag{11}$$

where $E_{{\rm u},j}^0/(hc)$ and $E_{{\rm l},j}^0/(hc)$ denote the eigenvalues in $\rm cm^{-1}$ for the upper and lower vibrational level, respectively. $\left|v_j\right\rangle$ denotes the vibrational eigenfunction of mode j in the absence of parity violation, respectively (see Eq. (8)). As can be seen from Eq. (11), the main quantity to be calculated is the expectation value of the parity violating potential for the upper and the lower vibrational state.

3. Results and discussion

Simple carbanions like ethyl or isopropyl are unstable in solution [82]. From simple C_1 carbanions, only CH_3^- has been observed in the gas phase. Carbanions can be generated by collision-induced decarboxylation of carboxylate negative ions [83]. They can be unstable with respect to loss of an electron and they need lifetimes toward electron detachment longer than 25 μs, to be detectable with flowing afterglow techniques [83]. Furthermore, the lifetime must compete with other reaction channels. CH_3^- has been proposed to have a pyramidal structure [82,84]. Carbanions can be products of a de-protonation in the gas phase. A number of experimental as well as theoretical investigations exist on electron affinities, heats of formation [84–86], and acidities [87–89]. If all substituents are different, $CRR'R''^-$ is chiral. One expects that reactions with chiral carbanions as intermediates should proceed with retention of configuration. This has, however, never been observed with carbanions that lack the possibility of resonance stabilization. The absence of retention in these compounds has been explained by rapid pyramidal inversion as in amines [90].

In the present study, various ab initio methods and different basis sets have been used to calculate the fully optimized geometry of (S)-$CBrClF^-$ which is depicted in Fig. 1 and the corresponding structural parameters are listed in Table 2. The geometric parameters seem to converge with basis set size up to augmented correlation consistent polarized valence quadruple zeta quality (aug-cc-pVQZ). The carbanion (S)-$CBrClF^-$ has a pyramidal structure. Additionally, we show the optimized geometry of the cation $CBrClF^+$ which is planar. The structural features of planar carbocations and pyramidal carbanions are well documented in the literature (see for example [82,84,91–95] and references therein).

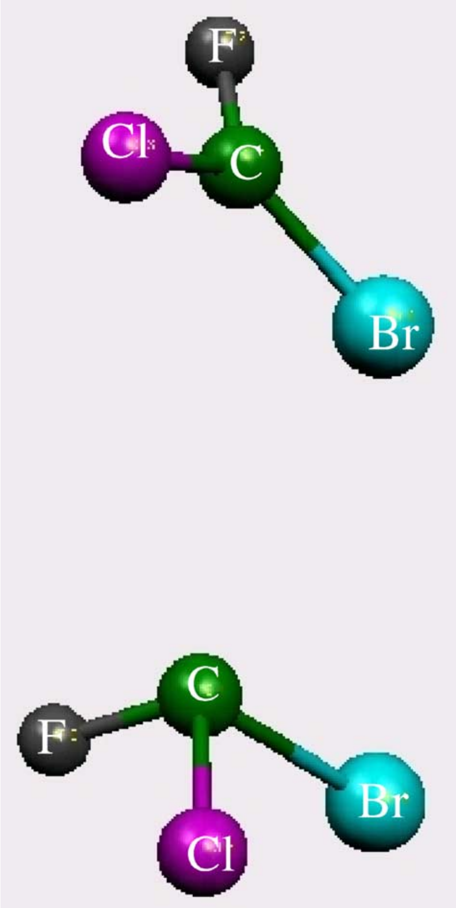

Fig. 1. Molecular geometry of the planar cation $CBrClF^+$ (top) and the pyramical anion (S)-$CBrClF^-$ (bottom) with labels carbon C(1), fluorine F(2), chlorine Cl(3) and bromine Br(4). The geometrical parameters are given in Table 2.

Table 3 summarizes the calculated harmonic vibrational frequencies $\tilde{\omega}_i$ in cm^{-1} and absorbance A_i in $km\,mol^{-1}$

Table 2

Fully optimized ab initio geometry (parameters are bond lengths, r, (Å), bond angles, α, and dihedral angle, δ, (°) and the rotational constants A, B, C are given in GHz) for the anion (S)-$CBrClF^-$ obtained with MP2 and DFT (B3LYP functional) methods

Parameter	$CBrClF^-$							
	MP2/A	MP2/B	MP2/C	MP2/D	B3LYP/A	B3LYP/(A+)	B3LYP/B	B3LYP/C
r(CF) (Å)	1.372	1.406	1.378	1.376	1.348	1.346	1.367	1.347
r(CCl) (Å)	1.944	1.941	1.915	1.904	1.979	1.967	1.977	1.974
r(CBr) (Å)	2.182	2.153	2.120	2.104	2.294	2.780	2.269	2.277
α(FCCl) (°)	101.7	101.1	101.6	101.7	101.8	101.9	101.4	101.8
α(FCBr) (°)	101.2	101.0	101.5	101.6	100.9	101.0	100.9	101.0
δ(BrCFCl) (°)	104.8	104.7	104.8	104.7	104.7	105.7	105.7	105.8
A (GHz)	6.1184	6.0612	6.2128	6.2482	6.0916	6.1274	6.0602	6.1144
B (GHz)	1.8286	1.8582	1.9198	1.9476	1.6752	1.6964	1.6993	1.6945
C (GHz)	1.4577	1.4751	1.5200	1.5388	1.3572	1.3724	1.3722	1.3706
$(E/E_h) + 3169$	−0.193726	−0.835358	−1.175914	−1.308769	−3.377796	−3.383465	−3.360835	−3.481194

The basis sets employed are: (A) 6-311+G(2d,2p), (A+) 6-311+G(2df,2pd), (B) aug-cc-pVDZ, (C) aug-cc-pVTZ, and (D) aug-cc-pVQZ. The last line lists the absolute energies in Hartree (E_h).

Table 3
Harmonic vibrational frequencies $\tilde{\omega}_i$ of mode i (in cm^{-1}) for the anion (S)-CBrClF^- obtained with MP2 and DFT (B3LYP functional) methods

Mode i	CBrClF^-						
	MP2/A	MP2/B	MP2/C	B3LYP/A	B3LYP/(A+)	B3LYP/B	B3LYP/C
$\mathrm{BrCCl_b}$	158.1 (9.3)	167.0 (7.2)	171.0 (6.4)	126.8 (11.8)	127.9 (13.1)	129.7 (12.5)	127.5 (11.6)
$\mathrm{BrCF_b}$	229.3 (36.8)	235.1 (30.8)	243.8 (27.1)	188.7 (64.1)	190.0 (63.8)	191.1 (59.8)	190.5 (64.5)
$\mathrm{ClCF_b}$	332.5 (32.5)	330.9 (26.5)	343.9 (25.2)	305.7 (57.1)	308.2 (56.9)	307.4 (48.6)	306.4 (54.8)
$\mathrm{CBr_s}$	497.3 (178.5)	508.2 (172.5)	524.7 (148.9)	439.3 (155.3)	441.8 (153.4)	443.8 (159.2)	442.1 (150.6)
$\mathrm{CCl_s}$	562.6 (135.3)	558.5 (130.0)	571.9 (132.6)	535.7 (111.6)	538.3 (109.8)	536.6 (109.2)	533.8 (99.9)
$\mathrm{CF_s}$	917.0 (248.9)	866.0 (212.4)	921.5 (214.8)	960.4 (277.4)	975.6 (274.6)	929.1 (253.4)	973.3 (263.4)

The basis sets employed are: (A) 6-311+G(2d,2p), (A+) 6-311+G(2df,2pd), (B) aug-cc-pVDZ, and (C) aug-cc-pVTZ. The numbers in parenthesis are intensities A_i (in $\mathrm{km\,mol^{-1}}$) which can be converted into the more suitable integrated band strength $G_i\ (\mathrm{pm}^2) \approx 16.60504[A_i\ (\mathrm{km\,mol^{-1}})]/[\tilde{\omega}_i\ (\mathrm{cm}^{-1})]$. The mode assignments in the first column are based on inspection of the displacement vectors; the labels s and b signify stretch and bend, respectively.

which can be converted to the more suitable integrated band strength $G_i\ (\mathrm{pm}^2) \approx 16.60504[A_i\ (\mathrm{km\,mol^{-1}})]/[\tilde{\omega}_i\ (\mathrm{cm}^{-1})]$ [96]. An approximate description of the vibrational motion belonging to each mode i is also given in the table. It is based on visual inspection of the vibrational displacement vectors [97].

We have determined the heats of reaction at $T = 0\,\mathrm{K}$ ($\Delta_r H_0^\circ$) for various reaction channels from the electronic energies E_e and the zero-point vibrational harmonic energy E_z ($2E_\mathrm{z} = \sum_i \tilde{\omega}_i(hc)$) according to [58].

$$\Delta_r H_0^\circ = \sum \nu_i E_\mathrm{e}(i) + \sum \nu_i E_\mathrm{z}(i) \tag{12}$$

with the stoichiometric coefficient ν_i of species i and the convention $\nu_i > 0$ for products and $\nu_i < 0$ for reactants. The chiral pyramidal carbanion (S)-CBrClF^- is energetically stable both with respect to electron detachment as well as to loss of Br^-:

$$\mathrm{CBrClF}^- = \mathrm{CBrClF} + \mathrm{e}^- \tag{13a}$$

$$\mathrm{CBrClF}^- = \mathrm{CClF} + \mathrm{Br}^- \tag{13b}$$

For the electron loss reaction (13a) we determined $\mathrm{EA} = \Delta_r H_0^\circ(13\mathrm{a}) = 231 \pm 5\,\mathrm{kJ\,mol^{-1}}$. EA denotes the electron affinity in the convention as used in [68]. In case of Eq. (13a) we adopted the “electron convention” and take the energy of the free electron equal to zero at all temperatures [68]. The reaction channel (13b) for the breaking of the C–Br bond gives for the differences of the electronic energies $\Delta_r E_\mathrm{e}(13\mathrm{b}) \approx 76 \pm 2\,\mathrm{kJ\,mol^{-1}}$ and $\Delta_r E_\mathrm{e}(13\mathrm{b}, \mathrm{CP}) = 61 \pm 2\,\mathrm{kJ\,mol^{-1}}$. The last value has been obtained by the standard counterpoise correction to deal with the basis set superposition error [98]. It has been shown that for ion/molecule reactions, the ambiguity of how the charge is distributed among the possible fragments seems to be of minor importance [99]. We used the distribution according to the products formed. With zero-point energy corrections, the heat of reaction is $\Delta_r H_0^\circ(13\mathrm{b}, \mathrm{CP\ mean}) \approx 67 \pm 2\,\mathrm{kJ\,mol^{-1}}$, where we have used the mean value of the electronic energies without and with counterpoise correction [100]. Further simple bond-fission reaction channels for the anion are

$$\mathrm{CBrClF}^- = \mathrm{CBrCl} + \mathrm{F}^- \tag{13c}$$

$$\mathrm{CBrClF}^- = \mathrm{CBrF} + \mathrm{Cl}^- \tag{13d}$$

with $\Delta_r H_0^\circ(13\mathrm{c}) \approx 295 \pm 5\,\mathrm{kJ\,mol^{-1}}$ and $\Delta_r H_0^\circ(13\mathrm{d}) \approx 124.5 \pm 5\,\mathrm{kJ\,mol^{-1}}$. A barrier to inversion has been estimated for a planar transition state to about $240 \pm 5\,\mathrm{kJ\,mol^{-1}}$ above the minimum structure and about $168\,\mathrm{kJ\,mol^{-1}}$ above the presumably lowest reaction channel Eq. (13b) which would then correspond to one real transition state for inversion as well by dissociation/recombination. A transition state for reaction (13b) could be located approximately $15\,\mathrm{kJ\,mol^{-1}}$ (mean between uncorrected and counterpoise corrected value) above the exit channel. This allows a cautious estimate of the time scale for uni-molecular dissociation on the order of ms or longer at room temperature (high pressure limit) [101]. De-protonation of CHBrClF

$$\mathrm{CHBrClF} = \mathrm{CBrClF}^- + \mathrm{H}^+ \tag{13e}$$

to form CBrClF^- leads to $\Delta_r H_0^\circ(13\mathrm{e}) = 1470 \pm 5\,\mathrm{kJ\,mol^{-1}}$ with $E_\mathrm{e}(\mathrm{H}^+) = 0\,\mathrm{kJ\,mol^{-1}}$. This fits into the series of methane and its fluorinated derivatives $\mathrm{CH_4}$, $\mathrm{CH_3F}$, $\mathrm{CH_2F_2}$, and $\mathrm{CHF_3}$ for which the heat of reaction for the deprotonation has been calculated (MP2, 6-31+G* basis; zero-point energy corrections on the level of Hartree–Fock) to be 1744, 1700, 1637, and $1543\,\mathrm{kJ\,mol^{-1}}$ [89]. The uncertainty in the heats of reaction as listed here follows from the use of different methods (MP2, DFT) with different basis sets (6-311+G(2d,2p) aug-cc-pVTZ).

Fig. 2 shows a vibrational potential energy V_0 as a function of the dimensionless reduced normal coordinate. It displays the CF-stretching co-ordinate for the anion with a Morse-like anharmonic potential shape. The vibrational potential shown here has been calculated using MP2 with the 6-311+G(2d,2p) basis set (termed A in Tables 2 and 3). The slightly larger basis 6-311++G(2d,2p) has been used to determine the parity violating potentials V_pv with the RPA within the multi-configurational linear response approach [45]. In contrast to CHBrClF and CDBrClF, CASSCF could not be used to check the quality of RPA. The largest active space with 14 electrons distributed in 14 orbitals was not yet sufficient to obtain results that were converged with respect to the size of the active space at geometries displaced from equilibrium. For some displacements, we found that

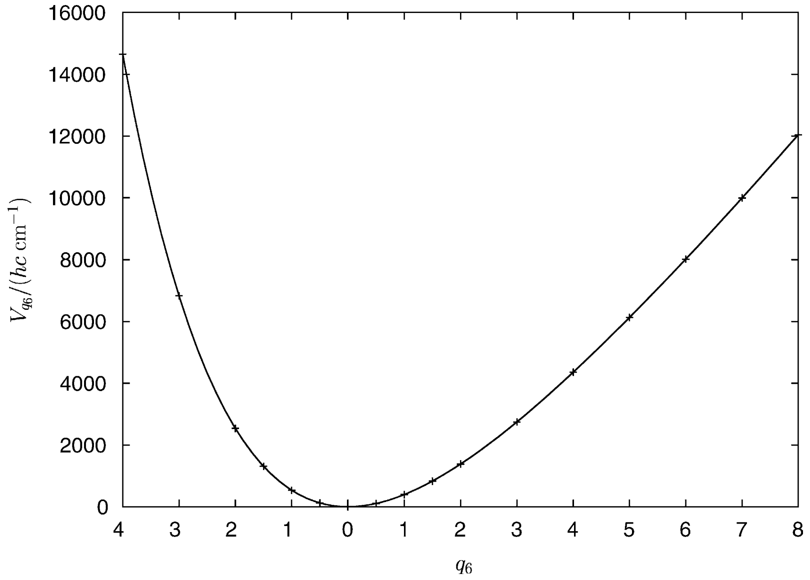

Fig. 2. One dimensional cut through the six-dimensional vibrational potential energy surface of $V(q_6)$ for the anion (S)-CBrClF$^-$ as a function of the corresponding dimensionless reduced normal coordinate.

the T$_1$-diagnostics [102] using the CCSD(T) method gives 0.015 (equilibrium) and 0.019 (displaced at $q_1 = -7$) which might indicate a breakdown of a single reference picture. We, therefore, made sure to not explore regions of the potential energy landscape where a single reference approximation to the electronic ground state might be expected to break down. The anharmonic frequency shifts have been obtained in the proximity of the equilibrium up to the first overtone to avoid the above mentioned difficulties. For each vibrational mode i, $V_{\mathrm{pv}}(q_i)$ has been fitted to a polynomial expansion in q_i of up to degree 8

$$V_{\mathrm{pv}}/(hc) = \sum_{i=0}^{8} \tilde{p}_i q_i^i \qquad (14)$$

We fitted polynomial expansion parameters $\tilde{p}_i$ (in cm^{-1}) to all parity violating potentials shown in Fig. 3 but listed only the parameters for two selected vibrational modes in Table 4. The quality of the fit for all potentials is very good with a standard deviation of the parameter (in units of the last significant digits) being much smaller than the magnitude of the parameter itself. The parameter $\tilde{p}_0$ should be equal for all modes within numerical uncertainties as it corresponds approximately to the energy difference between both enantiomers or to the enthalpy of reaction at $T = 0\,\mathrm{K}$, $\Delta_{\mathrm{pv}} H_0^\circ$, for racemization according to

$$\mathrm{R} \rightleftharpoons \mathrm{S}, \quad \frac{\Delta_{\mathrm{pv}} H_0^\circ}{hcN_{\mathrm{A}}} \approx \Delta_{\mathrm{pv}} E = 2\tilde{p}_0 \qquad (15)$$

where N_{A} is Avogadro's constant. The magnitude of $\tilde{p}_0$ is about 20% larger compared to CHBrClF$^-$ [51] but with different sign. Here, (S)-CBrClF$^-$ is more stable than (R)-CBrClF$^-$ (see Eq. (15) and Table 4) by about $-2.85 \times 10^{-11}\,\mathrm{J\,mol}^{-1}$, which is slightly larger in magni-

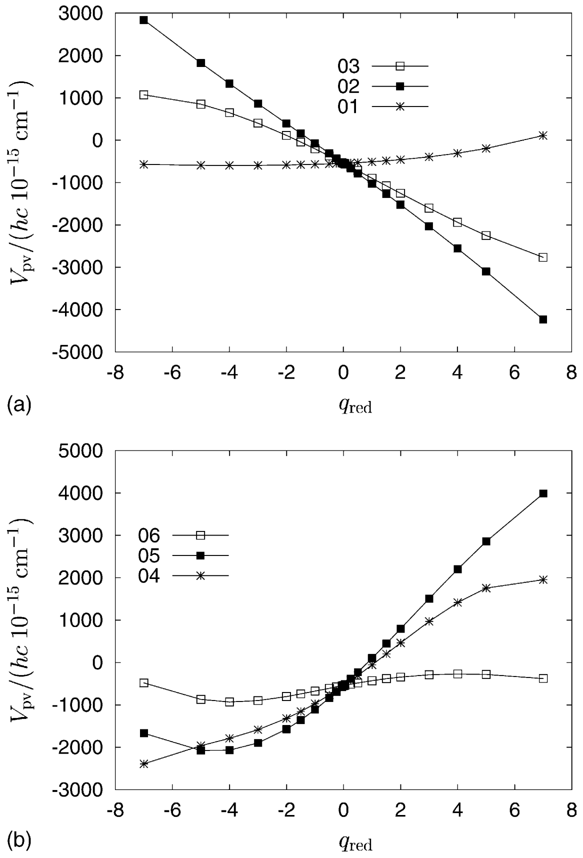

Fig. 3. Parity violating potential $V/(hc)$ in $10^{-15}\,\mathrm{cm}^{-1}$ for the anion (S)-CBrClF$^-$ as a function of the reduced normal coordinates q_{red} for the modes 1–3 (upper part) and 4–6 (lower part).

Table 4
Fitted polynomial parameters $\tilde{p}_i$ with $i = 0, \ldots, 8$ for the CF-stretching mode ν_6 and the BrCF-bending mode ν_2 in the anion (in units of $10^{-15}\,\mathrm{cm}^{-1}$)

Mode	Parameters in $10^{-15}\,\mathrm{cm}^{-1}$ for (S)-CBrClF$^-$									
	$\tilde{p}_0$	$\tilde{p}_1$	$\tilde{p}_2$	$\tilde{p}_3$	$\tilde{p}_4$	$\tilde{p}_5$	$\tilde{p}_6$	$\tilde{p}_7$	$\tilde{p}_8$	d_{rms}
ν_2	−1192.709 (5)	−1045.384 (5)	−10.511 (4)	−1.527 (1)	0.098 (1)	0.0050 (1)	−0.00052 (3)	–	0.0000129 (3)	0.010
ν_6	−1192.693 (73)	276.112 (85)	−19.310 (58)	−5.831 (16)	0.833 (8)	−0.014 (1)	−0.0075 (3)	0.00050 (1)	0.000013 (4)	0.164

The numbers in parentheses denote standard deviations in units of the last significant digits. The last column shows the root-mean-square d_{rms} of the fit.

Table 5
Relative frequency shifts $\Delta_{\mathrm{pv}}\tilde{x}_i/(\tilde{x}_i \times 10^{-19})$ in the separable harmonic (SHAA with $x = \omega$, see Eq. (10)) and in the anharmonic (SAAA, with $x = \nu$, see Eq. (11)) adiabatic approximation where $\tilde{\omega}_i$ and $\tilde{\nu}_i$ are the harmonic (see Table 3) and anharmonic wavenumbers, respectively

Mode	$\Delta_{\mathrm{pv}}\tilde{x}_i/(\tilde{x}_i \times 10^{-19})$						
	(S)-CBrClF$^-$			(S)-CHBrClF		(S)-CDBrClF	
	SHAA	SAAA	$\tilde{\nu}_i$ (cm^{-1})	SAAA	$\tilde{\nu}_i$ (cm^{-1})	SAAA	$\tilde{\nu}_i$ (cm^{-1})
1	1522.9	485.9	157.0	−450.1	240.5	−96.9	244.7
2	−916.9	9627.0	227.9	3360.7	327.1	2814.9	328.0
3	−833.9	−6374.7	330.5	−1809.5	437.3	−1450.7	437.3
4	2789.7	−1014.3	494.6	−952.9	679.8	−1167.3	642.2
5	3080.2	6663.2	560.7	2499.5	833.1	3134.0	786.7
6	−421.2	825.8	901.1	805.9	1080.3	1351.3 (2144.4)	1097.4 (1082.4)

Entries for (S)-CHBrClF and (S)-CDBrClF are from Table 4 [67] (multiplied by −1 because in [67] calculations have been performed for the R-enantiomer) and the value in parenthesis (last row) is from a four-dimensional fully coupled calculation (see [67]).

tude than the value obtained for (R)-CHBrClF (or CDBrClF) of about $+1.92 \times 10^{-11}\,\mathrm{J\,mol^{-1}}$ [67].

The fitted one-dimensional parity violating potential has then been used to determine the relative vibrational frequency shifts in the separable harmonic (SHAA) (see Eq. (10)) and in the anharmonic (SAAA) adiabatic approximation. In SAAA, the frequency shift is obtained from expectation values for the first vibrationally excited state and the vibrational ground state ($u = 1$, $l = 0$, as required by the expression shown in Eq. (11)). The vibrational Schrödinger equation has been solved numerically on a grid in a coordinate range for q_{red} from −7 to +7 except for the CF-stretching mode ν_6 where −4 to +8 has been used.

Table 5 shows the anharmonic relative frequency shifts calculated as described above. Except for the highest and the lowest modes $i = 1, 6$, the relative frequency shifts of the molecular carbanion (S)-CBrClF$^-$ are larger in magnitude than those obtained for CHBrClF [51]. The relative shifts depend strongly on the diagonal anharmonicity which can be seen by comparing harmonic (SHAA) and anharmonic (SAAA) relative shifts. We observe large changes in magnitude as well as in sign. It shows again that expectation values based on harmonic vibrational contributions alone can differ markedly from those that are based on more realistic anharmonic vibrational contributions. This might also be relevant for zero-point vibrational corrections recently computed for NMR parameters [103,104].

In Fig. 4 we display the parity violating potential of the carbocation CBrClF$^+$. There is only one vibrational out-of-plane mode which exhibits non-zero parity violating potential energy V_{pv}. Motion along q_4 shows vibrationally-induced parity violation. Upon fitting the parity violating potential. we find that only the parameters $\tilde{p}_i$ which are odd in q_4 are different from zero. Consequently, since the vibrational potential V_0 is symmetric with respect to q_4 and V_{pv} is anti-symmetric (in first-order perturbation theory), the expectation values are identical to zero and the planar carbocation CBrClF$^+$ does not show parity violation-induced relative frequency shifts, as expected.

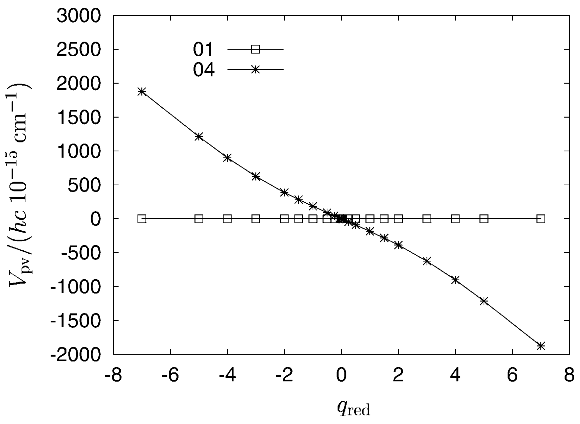

Fig. 4. Parity violating potential $V/(hc)$ in $10^{-15}\,\mathrm{cm}^{-1}$ for the cation CBrClF$^+$ as a function of the reduced normal coordinate q_{red}. For symmetry reasons there is only one vibrational mode (4, a'') for which V_{pv} is non-zero; all other totally symmetric modes (a') have a zero parity violating potential which is exemplified here for mode 1 (horizontal line).

4. Conclusions

We summarize the main findings of our investigation on the carbanion (S)-CBrClF$^-$ in view of parity violation in molecular ions. A planar transition structure is located at about 240 ± 5 kJ mol^{-1} above the minimum of the carbanion (S)-CBrClF$^-$. We anticipate that due to the high barrier, parity may dominate over tunneling [27]. Dissociation into Br$^-$ and CClF is endothermic by about 59 kJ mol^{-1} after counterpoise correction. (S)-CBrClF is also stable against electron loss by about 231 kJ mol^{-1}. (S)-CBrClF$^-$ should be stable and might be a candidate for spectroscopic investigation. Based on statistical uni-molecular rate theory with fixed transition state [101], we cautiously estimate the characteristic time scale for dissociation to be longer (about ms) than the lifetime required by the flowing afterglow technique (about μs). Again inversion would have to compete kinetically with the energetically much lower reaction channel Eq. (13b).

Our earlier investigation of molecular parity violation and its influence on observable spectroscopic quantities in CHBrClF and CDBrClF, and our findings presented here for CBrClF$^-$ suggest that parity violation-induced frequency shifts for this carbanion are larger in magnitude by up to a factor of three, depending on the vibrational mode considered. However, this is not the case for the CF stretching mode ν_6 (with an absorption close to CO$_2$-laser emission around 1000 cm^{-1}) where the relative frequency shift hardly changes when compared to the neutrals. This makes CBrClF$^-$ a less well suited candidate for the direct spectroscopic experimental determination of relative frequency shifts in the CF-stretching region as described in the first type of experiments (time-independent) in the introductory section. However, CBrClF$^-$ might be a candidate for the second type of experiment (time-dependent), as suggested by Quack [27,30].

We expect that couplings among the vibrational modes change the relative frequency shifts reported in Table 5. The work presented here will be extended by considering coupling between the vibrational modes either in an approximate way through the use of an effective reaction path ansatz [105–109] by explicitly considering all or in first place the most important couplings in a multi-dimensional treatment [112]. From previous investigations of Cl$_2$S$_2$ [109] it seems clear that CBrClF$^-$ is a case where parity violation dominates over tunneling.

Acknowledgements

I am grateful to Martin Quack who has inspired the Zürich project on molecular parity violation, for his generous support and encouragement as well as many discussions and criticism. Discussions with Robert Berger Tae-Kyu Ha, David Luckhaus, as well as with present members of the Quack group are also gratefully acknowledged. Financial support by the Alliance for Global Sustainability (AGS) and ETH Zürich as well as generously allocated computer time from CSCS (Manno), the computer center RZETH, and C^4 at ETH are gratefully acknowledged.

References

[1] A. Qayyum, C. Mair, W. Schustereder, P. Scheier, W. Hess, T.D. Märk, Chem. Phys. Lett. 372 (2003) 166.
[2] A.E. Litherland, Ann. Rev. Nucl. Part Sci. 30 (1980) 437.
[3] J.P. Maier, J. Phys. Chem. A 102 (1998) 3462.
[4] A. Pelc, W. Sailer, P. Scheier, M. Probst, N.J. Mason, E. Illenberger, T. Märk, Chem. Phys. Lett. 361 (2002) 277.
[5] E. Uggerud, Top. Curr. Chem. 225 (2003) 3.
[6] D. Schröder, H. Schwarz, Top. Curr. Chem. 225 (2003) 133.
[7] D.A. Wild, E.J. Bieske, Int. Rev. Phys. Chem. 22 (2003) 129.
[8] J.H. Bowie, Int. J. Mass. Spectrom. 212 (2001) 249.
[9] C. Aubry, J.L. Holmes, Int. J. Mass Spectrom. 200 (2000) 277.
[10] T.D. Märk, A.W. Castleman Jr., Adv. At. Mol. Phys. 20 (1985) 65.
[11] G. Savard, G. Werth, Ann. Rev. Nucl. Part Sci. 50 (2000) 119.
[12] P. Gill, G.P. Barwood, H.A. Klein, G. Huang, S.A. Webster, P.J. Blythe, K. Hosaka, S.N. Lea, H.S. Margolis, Meas. Sci. Technol. 14 (2003) 1174.
[13] A.N. Luiten (Ed.), Frequency Measurement and Control: Advanced Techniques and Future Trends, Springer, Berlin, 2001.
[14] K. Szymaniec, W. Chalupczak, S.N. Lea, D. Henderson, Acta Phys. Pol. B 33 (2002) 2173.
[15] T.D. Lee, C.N. Yang, Phys. Rev. 104 (1956) 254.
[16] C.S. Wu, E. Ambler, R.W. Hayward, D.D. Hoppes, R. Hudson, Phys. Rev. 105 (1957) 1413.
[17] E. Fermi, Nuovo Cimento 11 (1934) 1.
[18] B. Zel'dovich, Sov. Phys. JETP 9 (1959) 682.
[19] M.-A. Bouchiat, C. Bouchiat, Rep. Prog. Phys. 60 (1997) 1351.
[20] J. Sapirstein, in: P. Schwerdtfeger (Ed.), Relativistic Electronic Structure Theory: Part 1, Elsevier, Amsterdam, 2002, Chapter 9, p. 468.
[21] N. Fortson, Phys. Rev. Lett. 79 (1993) 2383.
[22] G.D. Sprouse, S. Aubin, E. Gomez, J.S. Grossman, L.A. Orozco, M.R. Pearson, M. True, Eur. Phys. J. A13 (2002) 239.
[23] Y. Yamagata, J. Theor. Biol. 11 (1966) 495.
[24] D. Rein, J. Mol. Evol. 4 (1974) 15.
[25] V. Letokhov, Phys. Lett. A 53 (1975) 275.
[26] M. Quack, Angew Chem. Int. Ed. Engl. 114 (2002) 4812.
[27] M. Quack, Angew Chem. Int. Ed. Engl. 28 (1989) 571.
[28] W.A. Bonner, Top. Stereochem. 18 (1988) 1.
[29] W.A. Bonner, Chirality 12 (2000) 114.
[30] M. Quack, Chem. Phys. Lett. 132 (1986) 147.
[31] R. Berger, Phys. Chem. Chem. Phys. 5 (2003) 12;
M. Quack, Faraday Discuss. Chem. Soc. 99 (1994) for the original idea of such a scheme, see caption to Fig. 1, p. 390.
[32] O. Kompanets, A. Kukudzhanov, V. Letokhov, L. Gervits, Opt. Commun. 19 (1976) 414.
[33] A. Bauder, A. Beil, D. Luckhaus, F. Müller, M. Quack, J. Chem. Phys. 106 (1997) 7558.
[34] C. Daussy, T. Marrel, A. Amy-Klein, C. Nguyen, C. Bordé, C. Chardonnet, Phys. Rev. Lett. 83 (1999) 1554.
[35] T. Marrel, M. Ziskind, C. Daussy, C. Chardonnet, J. Mol. Struct. 599 (2001) 195.
[36] M. Ziskind, C. Daussy, T. Marrel, C. Chardonnet, Eur. Phys. J. D10 (2002) 219.
[37] R. Harris, L. Stodolski, Phys. Lett. B78 (1978) 313.
[38] R. Harris, L. Stodolski, J. Chem. Phys. 74 (1981) 2145.
[39] D.W. Rein, R.A. Hegstrom, P.G.H. Sandars, Phys. Lett. A71 (1979) 499.
[40] R.A. Hegstrom, D.W. Rein, P.G.H. Sandars, J. Chem. Phys. 73 (1980) 2329.
[41] H. Kiyonaga, K. Morihashi, O. Kikuchi, J. Chem. Phys. 108 (1998) 2041.
[42] A. Bakasov, T.K. Ha, M. Quack, in: J. Chela-Flores, F. Rolin (Eds.), Proceedings of the Fourth Trieste Conference (1995), Chemical Evolution: Physics of the Origin and Evolution of Life, Dordrecht, Kluwer Academic Publishers, 1996, p. 287.

[43] A. Bakasov, T.K. Ha, M. Quack, J. Chem. Phys. 109 (1998) 7263.
[44] A. Bakasov, T.K. Ha, M. Quack, J. Chem. Phys. 110 (1999) 6081.
[45] R. Berger, M. Quack, J. Chem. Phys. 112 (2000) 3148.
[46] P. Lazzeretti, R. Zanasi, Chem. Phys. Lett. 279 (1997) 349.
[47] J.K. Laerdahl, P. Schwerdtfeger, Phys. Rev. A60 (1999) 4439.
[48] A. Hennum, T. Helgaker, W. Klopper, Chem. Phys. Lett. 354 (2002) 274.
[49] A. Shukla, B.P. Das, D. Mukherjee, Phys. Rev. A 50 (1994) 2096.
[50] R. Berger, in: P. Schwerdtfeger (Ed.), Relativistic Electronic Structure Theory: Part 2, Elsevier, Amsterdam, Chapter 5, in press.
[51] M. Quack, J. Stohner, Z. Phys. Chem. 214 (2000) 675.
[52] M. Quack, J. Stohner, Phys. Rev. Lett. 84 (2000) 3807.
[53] J. Stohner, A. Beil, H. Hollenstein, O. Monti, M. Quack, in: 37th IUPAC Congress and 27th GDCh Meeting, Berlin, Germany, August 14–19, 1999, Frontiers in Chemistry: Molecular Basis of the Life Sciences, p. 525, ISBN 3-924763-82-8.
[54] R. Berger, M. Quack, J. Stohner, Angew Chem. Intl. Ed. Engl. 40 (2001) 1667.
[55] P. Schwerdtfeger, J. Laerdahl, C. Chardonnet, Phys. Rev. A 65 (2002) 042508-1-042508-7.
[56] J.K. Laerdahl, P. Schwerdtfeger, H.M. Quiney, Phys. Rev. Lett. 84 (2000) 3811.
[57] R. Viglione, R. Zanasi, P. Lazzeretti, A. Ligabue, Phys. Rev. A62 (2000) 2516.
[58] M. Quack, J. Stohner, Chirality 13 (2001) 745.
[59] A.L. Barra, J.B. Robert, L. Wiesenfeld, Europhys. Lett. 5 (1988) 217.
[60] A.L. Barra, J.B. Robert, Mol. Phys. 88 (1996) 875.
[61] G. Laubender, R. Berger, Chem. Phys. Chem. 4 (2003) 395.
[62] A. Soncini, F. Faglioni, P. Lazzeretti, Phys. Rev. A 68 (2003) 033402-1-0033402-4.
[63] P. Jungwirth, L. Skála, R. Zahradník, Chem. Phys. Lett. 161 (1989) 502.
[64] F. Faglioni, P. Lazzeretti, Phys. Rev. E65 (2002) 011904.
[65] S.F. Mason, G.E. Tranter, Mol. Phys. 53 (1984) 1091.
[66] M. Gottselig, M. Quack, J. Stohner, M. Willeke, Int. J. Mass Spectrom. 233 (2004) 373.
[67] M. Quack, J. Stohner, J. Chem. Phys. 119 (2003) 11228.
[68] J.C. Rienstra-Kiracofe, G.S. Tschumper, H.F. Schaefer III, S. Nandi, G.B. Ellison, Chem. Rev. 102 (2001) 231.
[69] M.J. Frisch, G.W. Trucks, H.B. Schlegel, G.E. Scuseria, M.A. Robb, J.R. Cheeseman, V.G. Zakrzewski, J.A. Montgomery Jr., R.E. Stratmann, J.C. Burant, S. Dapprich, J.M. Millam, A.D. Daniels, K.N. Kudin, M.C. Strain, O. Farkas, J. Tomasi, V. Barone, M. Cossi, R. Cammi, B. Mennucci, C. Pomelli, C. Adamo, S. Clifford, J. Ochterski, G.A. Petersson, P.Y. Ayala, Q. Cui, K. Morokuma, P. Salvador, J.J. Dannenberg, D.K. Malick, A.D. Rabuck, K. Raghavachari, J.B. Foresman, J. Cioslowski, J.V. Ortiz, A.G. Baboul, B.B. Stefanov, G. Liu, A. Liashenko, P. Piskorz, I. Komaromi, R. Gomperts, R.L. Martin, D.J. Fox, T. Keith, M.A. Al-Laham, C.Y. Peng, A. Nanayakkara, M. Challacombe, P.M.W. Gill, B. Johnson, W. Chen, M.W. Wong, J.L. Andres, C. Gonzalez, M. Head-Gordon, F.S. Replogle, J.A. Pople, Gaussian 98, Rev. A.11.1, Gaussian Inc., Pittsburgh, PA, 2001.
[70] T. Helgaker, H. Jensen, P. Joergensen, J. Olsen, K. Ruud, H. Aagren, T. Andersen, K. Bak, V. Bakken, O. Christiansen, P. Dahle, F. Dalskov, T. Enevoldsen, B. Fernandez, H. Heiberg, H. Hettema, D. Jonsson, S. Kirpekar, R. Kobayashi, H. Koch, K. Mikkelsen, P. Norman, M. Packer, T. Saue, P. Taylor, O. Vahtras, DALTON, an Electronic Structure Program, release 1.0, 1997.
[71] A. Beil, H. Hollenstein, O. Monti, M. Quack, J. Stohner, J. Chem. Phys. 113 (2000) 2701.
[72] D. Luckhaus, M. Quack, Chem. Phys. Lett. 190 (1992) 581.
[73] A. Beil, D. Luckhaus, R. Marquardt, M. Quack, J. Chem. Soc. Faraday Discuss. 99 (1994) 49.
[74] D. Luckhaus, J. Chem. Phys. 113 (2000) 1329.
[75] R. Meyer, J. Chem. Phys. 52 (1970) 2053.
[76] M. Bouchiat, C. Bouchiat, J. Phys. 35 (1974) 899.
[77] M. Martinez, R. Miquel, L. Rolandi, R. Tenchini, Rev. Mod. Phys. 71 (1999) 575.
[78] T. Cvitaš, J. Frey, B. Holmström, K. Kuchitsu R. Marquardt, I. Mills. F. Pavese, M. Quack, J. Stohner, H.L. Strauss, M. Takami, A.J. Thor, Quantities, Units and Symbols in Physical Chemistry, IUPAC, in preparation.
[79] G.E. Tranter, Mol. Phys. 56 (1985) 825.
[80] A. Bakasov, M. Quack, Chem. Phys. Lett. 303 (1999) 547.
[81] A. Bakasov, R. Berger, T.-K. Ha, M. Quack, in press.
[82] M.B. Smith, J. March, March's Advanced Organic Chemistry: Reactions, Mechanisms, and Structure, 5 ed., Wiley, New York, 2001.
[83] S.T. Graul, R.R. Squires, J. Am. Chem. Soc. 112 (1990) 2506.
[84] H.M. Niemeyer, Tetrahedron 33 (1977) 2267;
J. Kalcher, A.F. Sax, Chem. Rev. 94 (1994) 2291;
J. Kalcher, R. Janoschek, Chem. Unserer Zeit. 33 (1999) 20.
[85] P.M. Mayer, L. Radom, J. Phys. Chem. A 102 (1998) 4918.
[86] R.R. Sauers, Tetrahedron 55 (1999) 10013.
[87] I.A. Koppel, J. Koppel, V. Pihl, I. Leito, M. Mishima, V.M. Vlasov, L.M. Yagupolskii, R.W. Taft, J. Chem. Soc. Perkin Trans. 2 (2000) 1125.
[88] P. Burk, K. Sillar, J. Mol. Struct. (Theochem.) 535 (2001) 49.
[89] H.J. Castejon, K.B. Wiberg, J. Org. Chem. 63 (1998) 3937.
[90] D.J. Cram, Fundamentals of Carbanion Chemistry, Academic Press, New York, 1965.
[91] D.G. Pratt, E. Rothstei, J. Chem. Soc. C—Org. 20 (1968) 2548.
[92] W. Zarges, M. Marsch, K. Harms, W. Koch, G. Frenking, G. Boche, Chem. Ber. 124 (1991) 543.
[93] A.M. Elnahas, P. von Schleyer, J. Comp. Chem. 15 (1994) 596.
[94] M.T. Jernigan, E.L. Eliel, J. Am. Chem. Soc. 117 (1995) 9638.
[95] U. Gross, D. Pfeifer, J. Fluor. Chem. 113 (2002) 17.
[96] M. Quack, J. Mol. Struct. 347 (1995) 245.
[97] P. Flükiger, H.-P. Lüthi, S. Portmann, J. Weber, MOLEKEL 4.2 Swiss Center for Scientific Computing, Manno (Switzerland), (2000–2002); S. Portman, H.P.-Lüthi, Chimia 54 (2000) 766.
[98] F.B. van Duijneveldt, J.G.C.M. van Duijneveldt-van de Rijdt, J.H. van Lenthe, Chem. Rev. 94 (1994) 1873.
[99] P. Salvador, M. Duran, J.J. Dannenberg, J. Phys. Chem. A 106 (2002) 6883.
[100] J.Y. Lee, S.J. Lee, H.S. Choi, S.J. Cho, K.S. Kim, T.-K. Ha, Chem. Phys. Lett. 232 (1995) 67.
[101] M. Quack, J. Troe, Statistical adiabatic channel model, in: P.v. Ragué Schleyer, N. Allinger, T. Clark, J. Gasteiger, P.A. Kollman, H.F. Schaefer III, P.R. Schreiner (Eds.), Encyclopedia of Computational Chemistry, vol. 4, John Wiley and Sons, 1998, p. 2708.
[102] T.J. Lee, P.R. Taylor, Int. J. Quant. Chem.: Quant. Chem. Symp. 23 (1989) 199.
[103] P.-O. Åstrand, K. Ruud, Phys. Chem. Chem. Phys. 5 (2003) 5015.
[104] K. Ruud, T. Helgaker, Chem. Phys. 296 (2004) 53.
[105] B. Fehrensen, D. Luckhaus, M. Quack, Z. Phys. Chem. N. F. 209 (1999) 1.
[106] B. Fehrensen, D. Luckhaus, M. Quack, Chem. Phys. Lett. 300 (1999) 312.
[107] W.H. Miller, N.C. Handy, J.E. Adams, J. Chem. Phys. 72 (1980) 99.
[108] M. Gottselig, D. Luckhaus, M. Quack, J. Stohner, M. Willeke, Helv. Chim. Acta 84 (2001) 1846.
[109] R. Berger, M. Gottselig, M. Quack, M. Willeke, Angew Chem. Intl. Ed. Engl. 40 (2001) 4195.
[110] E. Arimondo, P. Glorieux, T. Oka, Opt. Commun. 23 (1977) 369.
[111] H. Hollenstein, D. Luckhaus, J. Pochert, M. Quack, G. Seyfang, Angew Chem. Intl. Ed. 36 (1997) 140.
[112] J. Stohner, in preparation.